

Numerical Study of Turbulent Convective Cooling of Vertical Heat-Generating Rods Using Supercritical Water

M. Modir-Shanechi, M. Odabae, I. Bua and K.Hooman

School of Mechanical and Mining Engineering

The University of Queensland, QLD 4072, Australia

Abstract

Convection heat transfer in upward flows of supercritical water in rectangular tight rod bundles is numerically investigated using the commercially-available CFD software ANSYS Fluent© 15.

The heat-generating rod with an inner diameter of 10.2 mm and the pitch-to-diameter ratio (P/D) of 1.098 is studied for mass flux ranging between 550 and 1270 kg/m²s and heat flux of 560 kW/m² at pressures of 25 MPa.

V2F eddy viscosity turbulence model is used and, to isolate the effect of buoyancy, constant values are used for thermo-physical properties with Boussinesq approximation for the density variation with temperature in the momentum equations. The computed Nusselt number normalized by that of the same Reynolds number with no buoyancy against the buoyancy parameter proposed by Jackson and Hall's criterion.

A significant decrease in Nusselt number was observed in the range of $10^{-7} < Gr_q/Re_b^{3.425}Pr_b^{0.8} < 10^{-6}$ before entering a serious heat transfer deterioration regime. Based on an analysis of the shear-stress distribution in the turbulent boundary layer, it is found that the same mechanism that leads to impairment of turbulence production and thus heat transfer, in a vertical tube is present in square lattice heat-generating rod bundles at supercritical pressure.

Introduction

The supercritical pressure water-cooled reactor (SCWR) is an advanced nuclear reactor cooled with (light) water in its supercritical state. SCWR is a direct cycle nuclear system that operates under supercritical pressure conditions [15][1]. As is well known, when heated under sufficient pressure, water ceases to boil. The distinction between liquid and gaseous phases vanishes at pressures greater than 22.1 MPa and temperature of 648 K, known as the critical point. Above this temperature and pressure there is no phase change in water at supercritical pressure and also the thermo-physical properties of supercritical water vary continuously when temperature increases; however, strong variation in properties exist in the vicinity of the pseudo-critical temperature. The temperature at which the specific heat capacity is maximum, called the 'pseudo-critical temperature'. Among all sharp variations in properties, density variation brings large non-uniformity of buoyancy forces over the cross-section of channels resulting in complicated phenomenon called heat transfer deterioration (HTD) [14][2].

Figure 1 shows the variations of specific heat capacity and density near pseudo-critical temperature. Variation of the thermo-physical properties can affect transport phenomena in fluid flows, an effect that cannot be ignored in some cases. A good example is the case of fluids at pressures slightly higher than critical pressure where a rapid

variations in the values of specific heat, density, viscosity and thermal conductivity against temperature is present [1][3].

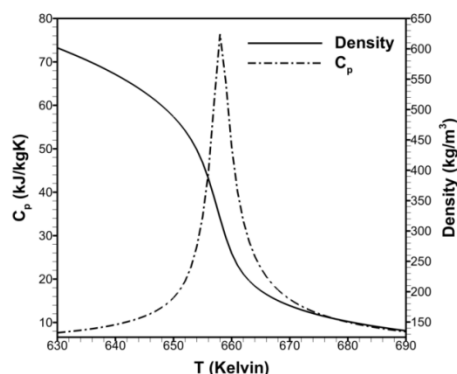


Figure 1. Variation of specific heat and density for supercritical water in 25 MPa

Variation of density can affect heat transfer also in a rather indirect manner, which is, causing significant buoyancy forces thereby changing the fluid's velocity field. As mentioned, a notable phenomenon stemming from this boost of buoyancy force is what commonly referred to as "heat transfer deterioration" or briefly "deterioration". Deterioration, which is simply a sudden reduction in the value of heat transfer coefficient, is likely to occur whenever the regime is turbulent, the flow direction is vertical and in the same direction as the buoyancy force adjacent to the wall, i.e. upward heating or downward cooling. In 1979, Jackson and Hall [7][4] explained this phenomenon as the indirect impact of buoyancy on the production of turbulence kinetic energy by deforming the velocity profile in a channel. According to their explanation, in an upward flow, heated fluid near the wall tends to move upward faster because it is lighter. As a result, the velocity profiles differs from that of the corresponding no-buoyancy flow so that the velocity gradient decreases in a region near the wall where turbulence production is expected to be significant otherwise. It reduces the level of turbulence intensity and, consequently, heat transfer is deteriorated. Aiming to predict the onset of deterioration, Jackson [8][5] introduced a buoyancy parameter (Bo) to quantify the buoyancy effect:

$$Bo = \frac{Gr}{Re^{3.425}Pr^{0.8}} \quad (1)$$

where

$$Gr = \frac{\rho_b^2 g \beta_b q_w d_h^4}{\mu_b^2 \lambda_b} \quad (2)$$

When this buoyancy parameter reaches a certain threshold, sudden decrease in the value of heat transfer coefficient, or Nusselt number, is observed. It must be noted that in very high values of buoyancy parameter, heat transfer starts to recover as a result of free

convection becoming dominant. This ‘deterioration’ and ‘recovery’ sequence can be seen in Figure 4. Further details about this graph are presented in following section.

As this phenomenon is closely related to the mechanism by which turbulence energy is produced, the right choice of turbulence model is crucial here. A widespread choice for this problem has been low Reynolds variations of $k-\epsilon$ model [2, 6, 11][6-8]. However, more careful studies have recently revealed that this class of two-equation models may not be as loyal to the physics of problem as their results suggest. The same references recommend a more elaborated four equation model of $k-\epsilon-v^2-f$ [3][9] to be the best choice within the category of eddy viscosity models [4-6, 9][7, 10-12].

The present paper, aims to investigate the deterioration phenomenon in square lattice rod bundles using Boussinesq assumption in order to isolate the effect of buoyancy on heat transfer in rectangular lattice rod bundles. This phenomenon is important for the designs of SCWRs, so the main purpose of this research is to investigate and explain the origin of this complicated phenomenon and to find the effect of buoyancy from the view point of heat transfer in turbulent flow.

Mathematical and physical modelling

Governing equations

One of the main issues in modelling mixed convection turbulent flows is the choice of the turbulence model. Due to their simplicity, Low-Reynolds $k-\epsilon$ models have been widely used for this problem. However, a weakness of these models is using artificial damping function to correct the value of eddy viscosity near wall. Mohseni et al. [12][13] suggested $k-\epsilon-v^2-f$ (V2F) model, a 4-equation eddy viscosity model, as a more reliable alternative. Other researches [4-6][7, 11, 12] also found V2F model a more consistent model for their problems of interest. Therefore, the V2F model is chosen for this study.

The details of governing equations for flow and heat transfer with $k-\epsilon-v^2-f$ model and the values of model constants are presented in [10, 13][14, 15].

Continuity:

$$\nabla \cdot \vec{U} = 0, \quad (3)$$

Momentum:

$$\nabla \cdot (\vec{U}\vec{U}) = -\frac{\nabla P}{\rho} + \vec{g}\beta(T - T_{ref}) + \nabla \cdot (2(\nu + \nu_t)S), \quad (4)$$

where \vec{U} is the Reynolds averaged velocity vector and $S = \frac{1}{2}(\nabla\vec{U} + \nabla\vec{U}^T)$. In this paper, constant properties are assumed along with Boussinesq approximation for Archimedes’ force term in the momentum equation as suggested by Kim et al. [9][10] in order to isolate the effects of buoyancy from other effects arising due to property variation.

Energy:

$$\nabla \cdot (\vec{U}h) = \nabla \cdot \left(\left(\frac{\nu}{Pr} + \frac{\nu_t}{Pr_t} \right) \nabla T \right). \quad (5)$$

The following constant values are used for the properties. These values are chosen close to those of water around its pseudo-critical point in 25 MPa, i.e. slightly above its critical pressure (22.064 MPa). Pseudo-critical point is a point where the variation of density is most rapid; hence deterioration is most likely to happen.

$$\rho = 510 \left(\frac{\text{kg}}{\text{m}^3} \right), \quad \lambda = 0.38 \left(\frac{\text{W}}{\text{mK}} \right)$$

$$\mu = 6 \times 10^{-5} (\text{Pa}\cdot\text{s}), \quad \beta = 0.1 (K^{-1})$$

On the solid walls, no-slip condition is applied for the velocity components while turbulence kinetic energy and velocity scale ($\overline{v^2}$) are both zero on the wall.

Constant heat flux boundary condition is applied on the wall and symmetry boundary conditions are assumed to reduce the computational time. Further details related to physical modelling will be given in the forthcoming discussion.

Physical modelling

The heat transfer in sub-channel of square lattice bundles are studied to provide detailed understanding of the heat transfer for design of SCWRs. In the core design of Super-LWR, rods are arranged around square rods in assemblies to get a homogeneous and sufficient moderation. For simplicity, square arrangement of rods in the bundles are studied. Because of the symmetric geometries and in order to save computing time, the sub-channel are taken as 1/8 of the whole sub-channel of the square lattice as shown in Figure 2.

In 2006, Yang et al. [14][2] investigated this geometry as the distribution of temperature to study the nonuniformity of the circumferential distribution of the cladding surface temperature in sub-channels of square lattice bundle and square lattice bundles.

Lattice	Square
Fuel rod diameter	10.2
Inlet temperature	573 K
Inlet mass flux	Ranging between 550 and 1050 kg/m ² s
P/D	1.098
Height	2m
Heat flux	560 kW/m ²
Hydraulic diameter	0.83mm

Table 1. Parameters of the square lattice bundle

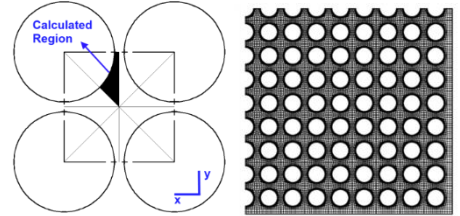


Figure 2. Schematic core assembly of square lattice bundles (right) and 1/8 of sub-channel of the square lattice (left)

On the symmetric boundaries, all flow quantities on one side of the boundaries are mirror images of those on the other side, and there are zero normal velocity and zero normal gradients for all other variables except for pressure. Parameters for square lattice bundle shown in

Solution of governing equations

Numerical scheme

Fluent, a finite volume-based commercial solver, is used for the CFD solution. SIMPLE scheme is adopted for coupling of momentum and continuity equations, and all fluxes are calculated using UPWIND method for better convergence except for the energy equation that second order method QUICK is employed.

The structured body-fitted mesh is used to fit the complex geometries with growth rate of 1.2 as depicted in Figure 3.

Mesh-independence analysis showed that the most critical mesh dimension is the thickness of the grid point adjacent to the wall, for which values of $y^+ < 2$ lead to mesh-independent results. The convergence criterion is that the residue tolerances are below 10^{-5} ,

including velocity components, mass, energy and turbulence parameters.

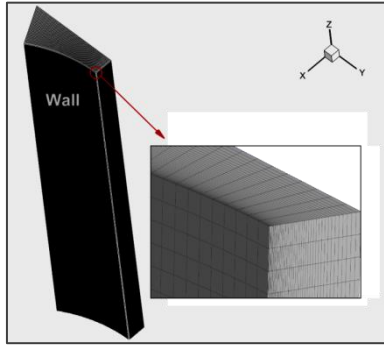


Figure 3. Scaled 3D mesh for calculated region

With lower computational cost of this approach, studying a wide range of parameters, which is expected from a screening study, became possible. It is, however, emphasized that the exploited turbulence model (V2F) is, based on the literature, the most reliable available model. This, to a high extent, guarantees that most of the physical trends can be captured satisfactorily. Further evidences on the validity of this simulation will be presented in the next section.

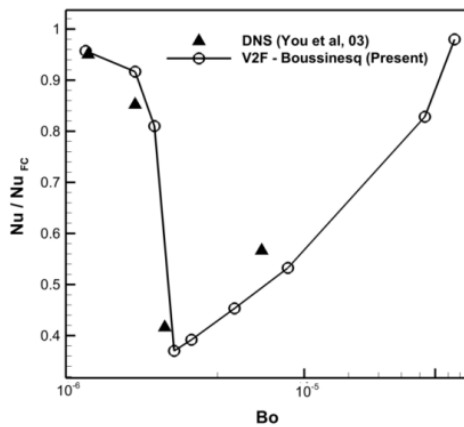


Figure 4. Variation of Nu/Nu_{Fc} against buoyancy parameter for vertical flow in $Re = 5300$ – comparison of the present results with DNS results [16][16]

Validation of results

Figure 4 shows the comparison of present result (V2F – Boussinesq approximation) with DNS data [24] where the variation of Nu/Nu_{Fc} against Bo is shown. As the Boussinesq assumption does not hold for real fluids, the best way of validating the present numerical solution is DNS data. However, the limitation of Reynolds number for DNS studies has made it impossible to find DNS results for the geometry of interest; as a result, DNS data for upward flow in heated vertical tubes are used for validation purpose. In this figure, on the ordinate is the ratio of the calculated Nusselt number to that of the forced convection under the same conditions (except for the buoyancy force term which is neglected). A sudden drop of Nusselt number is observed around $Bo = 2.5 \times 10^{-6}$ that can be considered the threshold for the buoyancy-induced heat transfer deterioration.

Verification of present numerical solution for lattice square rod bundles has been also assessed using the numerical results of Yang et al. [14][2] as Figure 5 shows. As seen, the variation of temperature distribution calculated by Boussinesq approximation against obtained data from Yang et al. [14][2] shows a similar trend. According to Figure 5, the results lie very close to each other, with the curve corresponding to present data shifting slightly to the right. This agrees with theory and shows the validity of the present numerical solution on lattice square fuel rod bundle.

Table 2 shows values of heat flux and mass that are used to obtain different values of buoyancy parameter in the present simulation. As the ratio of the heat flux to the mass flux is usually considered as a potential indicator of heat transfer deterioration, Table 2 is presented.

Bo	$q_w = 560 \text{ kW/m}^2$
	Mass Flux ($\text{kg/m}^2\text{s}$)
1.07×10^{-5}	550
6.78×10^{-6}	600
3.16×10^{-6}	750
1.69×10^{-6}	850
7.88×10^{-7}	1250

Table 2. Values of heat flux and mass flux for different buoyancy numbers at specified heat flux. The P/D is 1.14 mm and volumetric expansion is constant at (1/K)

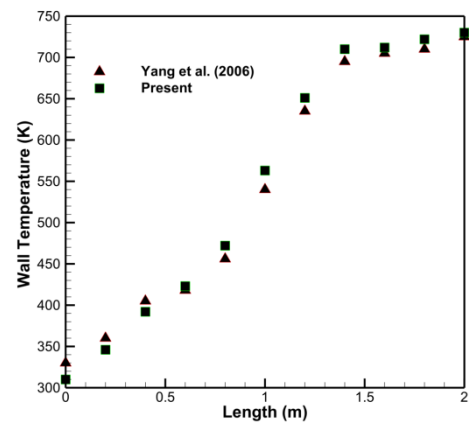


Figure 5. Distribution of temperature for vertical square lattice bundle – comparison of the present results with Yang et al. [14][2] results

Results and discussion

Observation of the velocity fields in different cases is a key to understand the trends observed in Figure 6. To do that, Figure 8 and Figure 9 are presented. Figure 8 depicts the distribution of axial velocity in a flow cross section in different buoyancy parameters for Boussinesq approximation. Figure 9 represents different values of Buoyancy parameter: $1.07E - 5$, a rather small value in which the departure from forced convection is still negligible; $3.16E - 6$, where deterioration is almost in its peak; $1.69E - 6$, where heat transfer is being recovered.

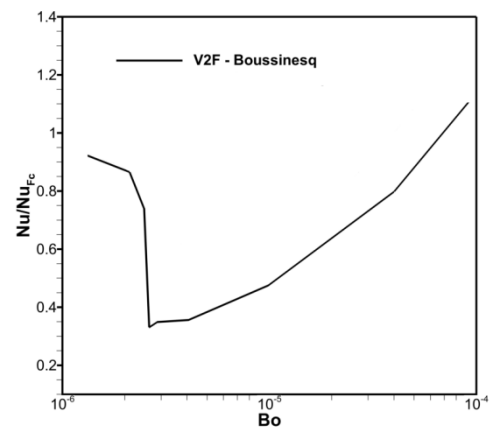


Figure 6. the ratio of calculated Nusselt number to forced convection Nusselt number against buoyancy parameter in square rod bundle

According to Figure 8, as Bo increases, the peak of velocity profile moves closer to the heated wall. It is obviously a result of Archimedes forces pushing the lighter near-wall fluid upward.

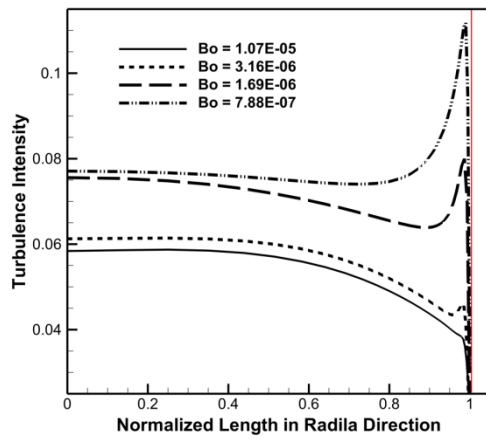


Figure 7. Profiles of turbulence intensity for flow in a square rod bundle with different Bo values

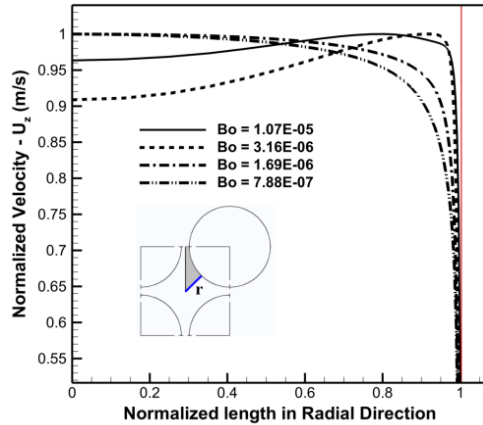


Figure 8. Profiles of axial velocity for flow in a square rod bundle with different Bo values

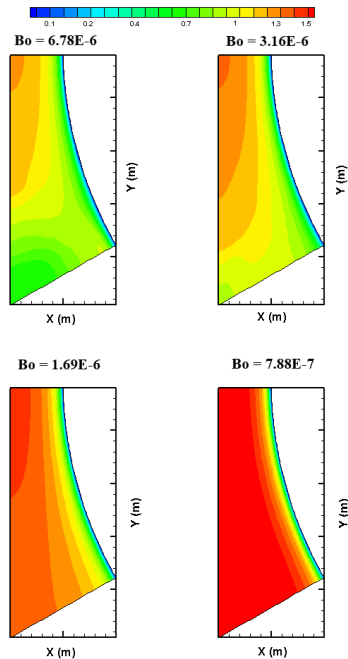


Figure 9. Axial velocity distribution for square lattice bundle in outlet. Four different buoyancy conditions are considered

When forced convection is dominant, the peak of velocity happens in the widest part of the cross section. As the contribution of free convection increases, it is observed that bigger portions of flow pass through the centre of the cross section. Eventually, for very big values of buoyancy parameter, the velocity peak moves away from the heated walls. Such a change in the velocity distribution is underlain by a change in the driving force of the flow. In the forced convection flow, the driving force is the pressure gradient; obviously with the same pressure drop, the fluid velocity is higher away from

the walls. On the other hand the, in ultimate case of free convection; the driving force is the Archimedes force adjacent to the heated wall leading to secondary flows.

As observed in Figure 8 when the Buoyancy number is around 1.07×10^{-5} , due to upward Archimedes' forces, an M-shape profile starts to develop. Such a change in the velocity profile leads to a decrease in the rate of the turbulence production and, thus, the turbulence intensity. As a result of formation of the M-shape velocity profile, the two last curves in Figure 7 are clearly different from the first two, as the near-wall peak disappeared.

This agrees well with Jackson's theory discussed above: the formation of velocity peak in the region where turbulence production is expected to be maximum leads to impairment of turbulence production and, as a result, heat transfer due to eddy diffusion will be suppressed.

Conclusion

Turbulent upward flow, with significant buoyancy effects, through square lattice bundle, was investigated. V2F turbulent model with Boussinesq approximation was used. To summarize the findings, it can be mentioned that:

- (1) Buoyancy-induced deterioration of heat transfer, similar to what observed in circular pipe, is also observed in the square lattice fuel rod bundle. The underlying deterioration mechanism is similar to that of a vertical circular pipe, i.e. impairment of turbulence production due to change in velocity gradient near the fuel rods.
- (2) The mechanism of deterioration can be explained by the theory of Jackson [7][4], which, in brief, states that the level of turbulence production decreases when axial velocity profile peaks near the heated wall due to buoyancy force.

References

- [1] Y. Y. Bae, H. Y. Kim, and D. J. Kang, "Forced and mixed convection heat transfer to supercritical CO₂ vertically flowing in a uniformly-heated circular tube," *Experimental Thermal and Fluid Science*, vol. 34, pp. 1295-1308, 2010.
- [2] M. Bazargan and M. Mohseni, "The significance of the buffer zone of boundary layer on convective heat transfer to a vertical turbulent flow of a supercritical fluid," *Journal of Supercritical Fluids*, vol. 51, pp. 221-229, 2009.
- [3] M. Behnia, S. Parneix, and P. A. Durbin, "Prediction of heat transfer in an axisymmetric turbulent jet impinging on a flat plate," *International Journal of Heat and Mass Transfer*, vol. 41, pp. 1845-1855, 1998.
- [4] Z. X. Du, W. S. Lin, and A. Z. Gu, "Numerical investigation of cooling heat transfer to supercritical CO₂ in a horizontal circular tube," *Journal of Supercritical Fluids*, vol. 55, pp. 116-121, Nov 2010.
- [5] P. Foroughi, R. Xu, P. X. Jiang, and K. Hooman, "Numerical simulation of convective heat transfer for supercritical CO₂ in vertical pipes using V2F turbulence model," presented at the 18th Australian Fluid Mechanics Conference, Launceston, Australia, 2012.
- [6] S. He, W. S. Kim, and J. H. Bae, "Assessment of performance of turbulence models in predicting supercritical pressure heat transfer in a vertical tube," *International Journal of Heat and Mass Transfer*, vol. 51, pp. 4659-4675, 2008.
- [7] J. D. Jackson and W. B. Hall, "Influence of buoyancy on heat transfer to fluids flowing in vertical tubes under turbulent condition," in *Turbulent forced convection in channels and bundles*, S. Kakac and D. B. Spalding, Eds., ed: Hemisphere Publishing, 1979, pp. 613-640.
- [8] J. D. Jackson, M. A. Cotton, and B. P. Axcell, "Studies of mixed convection in vertical tubes," *International Journal of Heat and Fluid Flow*, vol. 10, pp. 2-15, 1989.
- [9] W. S. Kim, S. He, and J. D. Jackson, "Assessment by comparison with DNS data of turbulence models used in simulations of mixed convection," *International Journal of Heat and Mass Transfer*, vol. 51, pp. 1293-1312, Mar 2008.
- [10] F.-S. Lien and G. Kalitzin, "Computations of transonic flow with the v2-f turbulence model," *International Journal of Heat and Fluid Flow*, vol. 22, pp. 53-61, 2// 2001.
- [11] D. P. Mikielewicz, A. M. Shehata, J. D. Jackson, and D. M. McEligot, "Temperature, velocity and mean turbulence structure in strongly heated internal gas flows: Comparison of numerical predictions with data," *International Journal of Heat and Mass Transfer*, vol. 45, pp. 4333-4352, 2002.
- [12] M. Mohseni and M. Bazargan, "The effect of the low Reynolds number k-ε turbulence models on simulation of the enhanced and deteriorated convective heat transfer to the supercritical fluid flows," *Heat and Mass Transfer*, vol. 47, pp. 609-619, 2011/05/01 2011.
- [13] A. Sveningsson and L. Davidson, "Assessment of realizability constraints in v2-f turbulence models," *International Journal of Heat and Fluid Flow*, vol. 25, pp. 785-794, 10// 2004.
- [14] J. Yang, Y. Oka, Y. Ishiwatari, J. Liu, and J. Yoo, "Numerical investigation of heat transfer in upward flows of supercritical water in circular tubes and tight fuel rod bundles," *Nuclear Engineering and Design*, vol. 237, pp. 420-430, 2// 2007.
- [15] J. Yoo, Y. Oka, Y. Ishiwatari, J. Yang, and J. Liu, "Subchannel analysis of supercritical light water-cooled fast reactor assembly," *Nuclear Engineering and Design*, vol. 237, pp. 1096-1105, 5// 2007.
- [16] J. You, J. Y. Yoo, and H. Choi, "Direct numerical simulation of heated vertical air flows in fully developed turbulent mixed convection," *International Journal of Heat and Mass Transfer*, vol. 46, pp. 1613-1627, 4// 2003.